JOURNAL OF OPTOELECTRONICS AND ADVANCED MATERIALS, Vol. 10, No. 9, September 2008, p. 2328 – 2333

Revealing nanoscale structural ordering by TEM/HRTEM. Application on PMN-PT relaxor ferroelectric

C. GHICA[a*], L. NISTOR[a], G. VAN TENDELOO[b]
[a]*National Institute of Materials Physics, Atomistilor 105 bis, 077125 Magurele, Ilfov, Romania*
[b]*University of Antwerp, Groenenborgerlaan 171, B-2020 Antwerpen, Belgium*

Nano-scale ordering may be revealed in transmission electron microscopy (TEM) by at least three techniques that will be presented in this work: selected area electron diffraction, conventional TEM and high-resolution TEM. Digital image processing is used to extract additional information from the high-resolution micrographs. The described methods are illustrated in a microstructural and compositional study of a 90%$Pb(Mg_{1/3}Nb_{2/3})O_3$-10%$PbTiO_2$ ceramic sample. High-resolution images reveal the presence of ordered compositional nano-domains, observable in two specific crystallographic orientations. Antiphase boundaries lying in the (111) planes separate them, while (100) and (111) facets separate the ordered domains from the disordered matrix.

(Received February 25, 2008; accepted August 14, 2008)

Keywords: Transmission electron microscopy, Digital image processing

1. Introduction

Transmission electron microscopy, by its various techniques, is undoubtedly the most powerful characterization method to reveal structural information at a nanometric scale. By appropriately manipulating the electron beam in the microscope, one may have access to structural crystallographic information (electron diffraction techniques and High Resolution Transmission Electron Microscopy – HRTEM), to the presence and microstructure of the crystallographic defects and interfaces (Conventional Transmission Electron Microscopy – CTEM, and HRTEM), to morphological information regarding the size and shape of nanocrystals (CTEM/HRTEM), and to compositional information (Energy Dispersive X-ray Spectroscopy – EDS, Electron Energy Loss Spectroscopy – EELS). The spatial resolution goes down to 0.1 nm for the most advanced aberration corrected microscopes in the HRTEM mode and to 1 nm in the analytical mode.

Nano-scale ordering may be revealed in transmission electron microscopy by at least three techniques that will be presented hereafter: selected area electron diffraction (SAED), CTEM and HRTEM. A digital image processing technique based on Fourier filtering is used in order to extract additional information from the HRTEM micrographs [1]. The described methods are illustrated in a microstructural and compositional study of a 90% $Pb(Mg_{1/3}Nb_{2/3})O_3$ - 10% $PbTiO_2$ ceramic sample [2]. $Pb(Mg_{1/3}Nb_{2/3})O_3$ is an outstanding relaxor ferroelectric material which exhibits a very high dielectric constant, high electrostrictive coefficients and a diffuse and dispersive phase transition over a temperature range near -15^oC [3, 4], too low for practical purposes. To increase the Curie temperature, solid solutions of PMN-PT have been reported [5], covering a wide range of applications depending on the amount of $PbTiO_3$ (PT). PMN-PT solid solutions with PT < 35% have the ABO_3 perovskite structure, space group Pm-3m, where different atomic species share the same crystallographic B-positions; the relaxor behaviour is due to the presence of nano-structural heterogeneities, consisting in a partial ordering of B-cations in nanometric domains [5-8]. HRTEM images reveal the presence of ordered compositional nano-domains (2 - 4 nm), observable in two specific crystallographic orientations, [0-11] and [11-2]. However, the visibility on the HRTEM images and the ordering degree of the nano-domains are not at all obvious. By Fourier filtering these images, we could clearly reveal the ordered domains.

2. Experimental

Before presenting the structural results on PMN-PT, we will briefly remind three basic operating modes of an electron microscope, based on the schematic representation of an electron microscope shown in Fig. 1. In this simple intuitive diagram, we have reduced the optical scheme of the microscope to its essential components in order to represent the image formation on the screen. We have illustrated the specimen, the objective lens of the microscope, the objective aperture, disposed in the back focal plane of the objective lens, and the imaging screen. After crossing the specimen, the incident electron beam splits in a transmitted beam (the most intense) and a series of diffracted beams, depending on the crystalline structure and orientation of the specimen. The way that the transmitted and diffracted beams are manipulated using the objective aperture and the projector lens system of the microscope (not included in the drawing) is at the base of three microstructural characterization techniques known as

Selected Area Electron Diffraction (SAED), Conventional Transmission Electron Microscopy (CTEM) and High-Resolution Transmission Electron Microscopy (HRTEM). Like in the case of an optical lens, the intensity distribution of the electron beam in the back focal plane represents the Fourier transform of the exit wave emerging from the specimen. This is the diffraction pattern of the specimen, which may look like a 2D periodic distribution of diffraction spots for single crystals, a set of concentric diffraction rings for polycrystalline specimens or a set of diffuse rings for amorphous structures. Using the objective aperture, one can select one or more diffracted beams in order to project the enlarged image of the specimen on the imaging screen. By selecting the transmitted beam only (Fig. 1a), all the diffracted beams will be obstructed and the image on screen displays *dark contrast* for the regions in the specimen satisfying the Bragg condition and bright contrast for the non-diffracting regions (non-oriented crystals, amorphous regions, holes). This operating mode represents the Bright Field Imaging (BFI). By selecting a diffracted beam with the objective aperture (Fig. 1b), one can reveal the sample regions contributing electrons to the selected diffracted beam. These regions will appear bright on a dark background in what is known as Dark Field Image (DFI). The three mentioned observation modes, SAED, BFI and DFI make up what is known as Conventional Transmission Electron Microscopy.

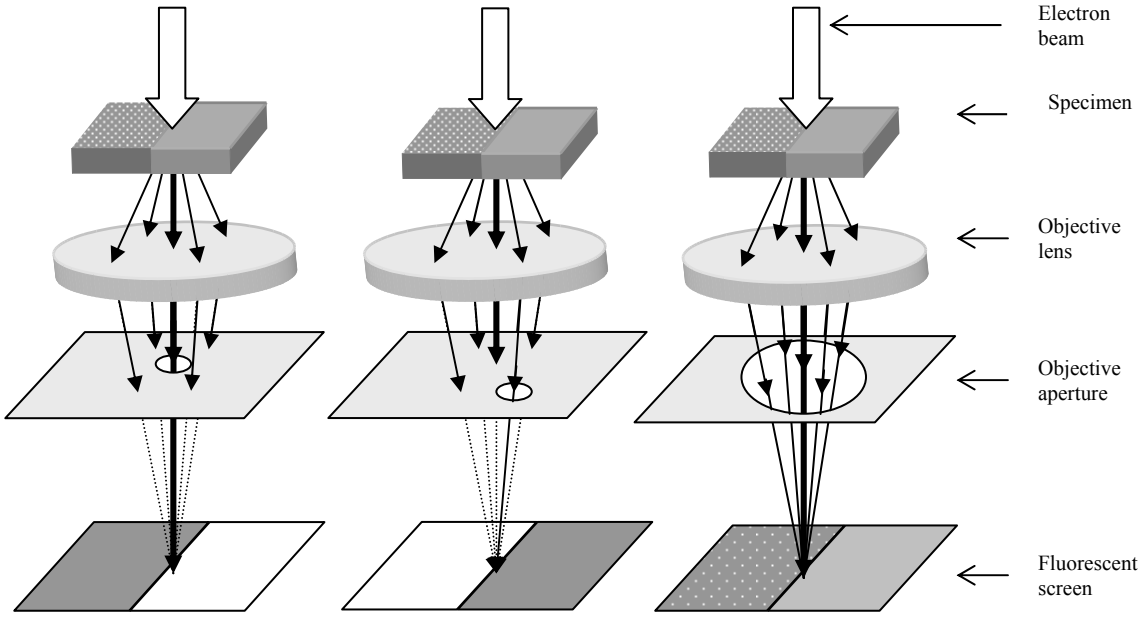

Fig.1. Three types of TEM contrast for a specimen including a crystalline region (left half) and an amorphous region (right half): (a) bright-field image; (b) dark-field image; (c) phase contrast, high-resolution image.

Using a larger aperture, one can select several diffracted beams in order to form the image on screen (Fig. 2c). Due to the high spatial coherency of the electron beam, the transmitted and diffracted electron beams, selected by the objective aperture, interfere and generate an interference pattern on screen, consisting in parallel bright/dark fringes. The fringe separating distance is directly related to the inter-planar distance characterizing the crystal planes generating the employed diffraction spots. This interference contrast is due to the phase difference between the beams contributing to the image reconstruction; this is why it is known as *phase contrast*. The electron microscopy field dealing with this kind of images represents the High-Resolution Transmission Electron Microscopy.

This short description of the basic operation modes of a TEM will be helpful for a better understanding of the way the ordering in PMN-PT at nanometric scale can be evidenced by electron diffraction, HRTEM and HRTEM image processing.

A commercial 0.9PMN - 0.1PT sintered pellet from TRS-Ceramics, USA, has been used in this study. Samples for transmission electron microscopy were obtained by crushing the material in alcohol and dispersing the fragments on holey carbon grids. HRTEM studies were performed with a JEOL 4000 EX electron microscope with a point resolution of 0.17 nm. HRTEM images were processed using the specialized Fourier filtering routines of the Digital Micrograph^{TM} 3.3 software.

3. Results and discussion

The diffraction patterns from grains oriented along two main zone axis, [01-1] and [11-2], are displayed in Fig 2. From the pattern indexation, one can identify the cubic perovskite crystal structure, space group Pm-3m, a=0.407 nm, typical for the $PbMg_{0.33}Nb_{0.67}O_3$ compound. After a careful inspection of the micrographs, one can notice the

presence of diffuse spots in the ½ 111 positions. It suggests a process of ordering in the (111) planes leading to the period doubling along the {111} directions and, implicitly, doubling of the cell parameter. The symmetry is locally modified to Fm-3m. From the diffuse aspect of the superstructure spots, one can deduce that the ordering phenomenon is not complete, but it occurs in small size domains.

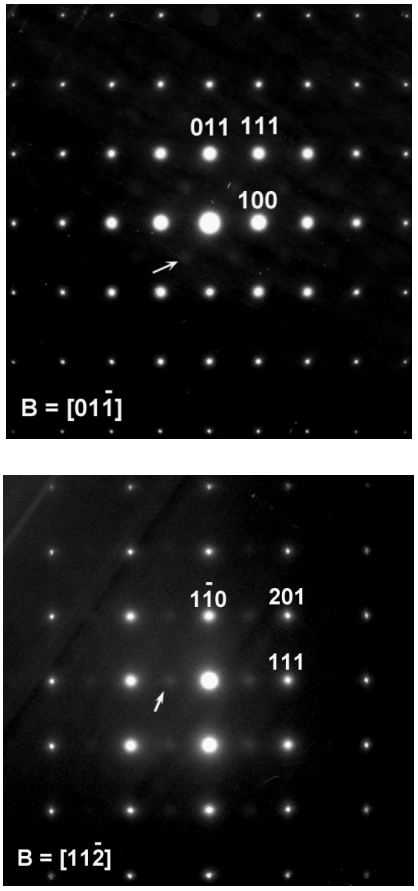

Fig. 2. Electron diffraction patterns along the [01-1] and [11-2] zone axes indexed with the Pm-3m perovskite structure. The weak diffuse spots at positions ½(111) are marked with arrows.

A major problem is to visualise the ordered domains and their boundaries and to estimate their size and volume fraction. The attempt to image these ordered domains by the means of the CTEM through dark field imaging was unsuccessful due to two reasons: i. the intensity of the superstructure spots was extremely low, which would have generated dark filed images with very low contrast; ii. the size of the ordered domains is in the nanometric range, which is close to the resolution limit in this observation mode. A better understanding of the local ordering due to compositional inhomogeneity of the relaxor perovskite can be performed by HRTEM. Since the sizes of the ordered domains are very small (2-4 nm), HRTEM observations were performed in the thinnest parts of the specimen in order to avoid the overlapping of the ordered and disordered regions. Since the unit cell of these nano-domains is doubled, i.e. $2a_0$ x $2a_0$ x $2a_0$ compared to a_0 x a_0 x a_0 for the normal perovskite cell, antiphase boundaries are expected to occur in the ordered phase.

HRTEM images of crystal grains oriented along the [01-1] and [11-2] zone axes are displayed in Fig. 3 (a) and (b), respectively. The ordered domains can be only be noticed by a careful examination at grazing incidence of the images. In order to clearly reveal the ordered domains and to get useful information about their size and distribution, we applied a digital image processing method based on Fourier filtering. The method, widely described by Hÿtch et al. in [1], is at the origin of specialized routines included in the Digital Micrograph^{TM} software that we used in this case.

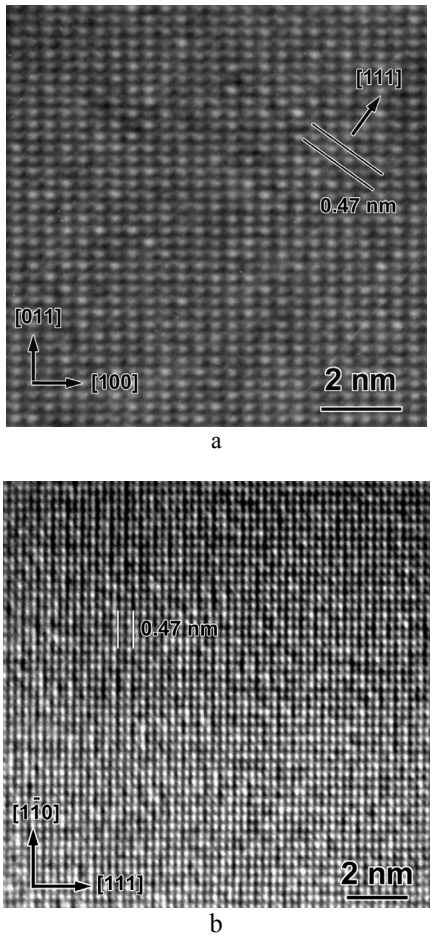

Fig. 3. HRTEM image from crystal grains oriented along the [01-1] zone axis (a) and [11-2] zone axis (b).Nanometric domains are observable, where the period along <111> doubles from 0.23 nm to 0.47 nm.

According to this processing method, the HRTEM image represents a 2D periodic intensity distribution that can be mathematically described by a Fourier series of the kind:

$$I(r) = \Sigma_g I_g(\mathbf{r})\exp(2\pi i\, \mathbf{g}\cdot\mathbf{r})$$

where $I_g(r)$ represent the Fourier complex components of the intensity $I(r)$, characterized by amplitude and phase:

$$I_g(\mathbf{r}) = A_g(\mathbf{r})\exp(i\, P_g(\mathbf{r}))$$

Both the amplitude and phase of the Fourier components are function of position ***r*** in the HRTEM image. The amplitude $A_g(\mathbf{r})$ represents the local contrast of the HRTEM image (i.e. how bright the white fringes are), while the phase of the Fourier components is related to the local relative position of the HR fringes with respect to a reference area chosen on the HR image. Based on this mathematical formalism, one can extract images where ordered domains, their ordering degree and size, phase relation between them can be revealed. We have applied this formalism to the images in Fig. 3 (a) and (b).

The Fourier transform of the image in Fig. 4 (a) is presented in Fig. 4 (b). Obviously, the obtained spectrum is identical with the diffraction pattern obtained in the electron microscope from the corresponding crystal grain (Fig. 2 a). Just like in the diffraction pattern, on the Fourier transform one can notice the presence of superstructure diffuse spots in the ½ (111) positions, suggesting the existence of small-size ordered domains. By selecting with an appropriate mask one of the superstructure spots (encircled in Fig. 4 b) one can generate, by inverse Fourier transform, an *amplitude image*. This image, presented in Fig. 4 (c), represents the distribution of the local amplitude $A_g(\mathbf{r})$ of the HR fringes corresponding to the $2d_{111}$ distance, the double of the d_{111} interplanar distance. The image amplitude displays in levels of gray areas with high/low amplitude of the $2d_{111}$ fringes, revealing this way the ordering degree inside the domains. Thus, on the amplitude image, bright represents areas of high amplitude and, implicitly, high ordering degree. Dark represents non-ordered areas, where period doubling does not occur. As one can notice, the size of the ordered domains is between 2-5 nm, while their shape is rather irregular. This image processing method is, in principle, analogue to the dark field imaging in the electron microscope. The advantage is that by Fourier filtering one can clearly reveal domains of nanometric dimensions, with a resolution inaccesible to the dark field technique. Interesting aditional results are obtained by selecting pairs of opposite superstructure spots from the Fourier transform image, or even the 4 visible superstructure spots. By inverse Fourier transform back to real space, sets of parallel fringes are obtained, separated at $2d_{111}$ distance (Fig. 4 d-f). Areas where fringes show the highest contrast coincide, obviously, with the brightest areas in the amplitude image (Fig. 4 c).

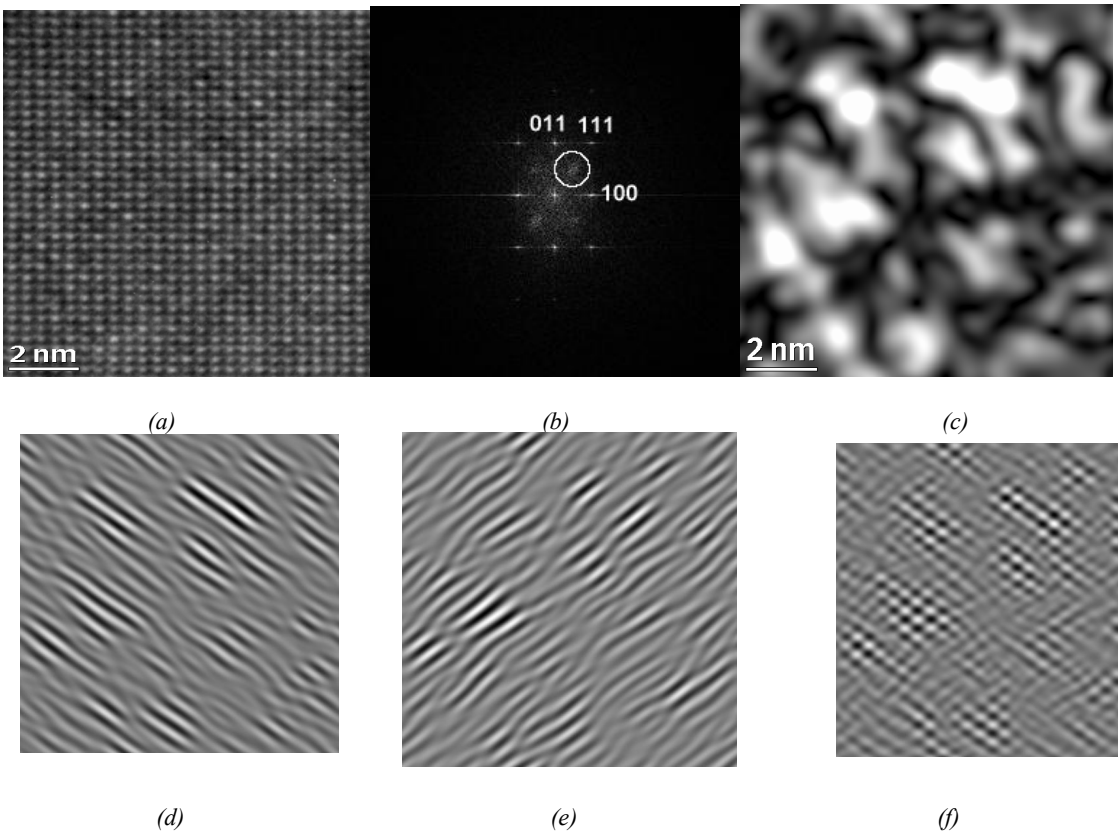

Fig. 4 (a) HRTEM image along the [01-1] zone axis; (b) FFT of the HRTEM image in (a); (c) amplitude image obtained from the FFT^{-1} of the distribution in (b) by selecting the diffuse spot in the ½ 111 position; (d) Fourier filtered image obtained by FFT^{-1} of the spectrum in (b) by selecting the diffuse spots ½½½ and -½-½-½; (e) Fourier filtered image obtained by FFT^{-1} of the spectrum in (b) by selecting the diffuse spots -½½½ and ½-½-½; (f) Fourier filtered image obtained by FFT^{-1} of the spectrum in (b) by selecting all 4 diffuse spots in the ½ 111 positions.

Figures 4d and 4e clearly reveal the antiphase relation existing between neighbouring ordered domains. The antiphase boundaries (APB) are oriented along the (111) planes separating the ordered domains. A strong bending of the lattice planes at the boundary between the ordered and the disordered regions is visible proving that these

regions are highly defected. The lattice planes are strained by the presence of the ordered domains. In regions between ordered and disordered domains, strong composition fluctuation should exist. Most probable at these interdomain boundaries, polar nano-clusters or quenched random electric fields responsible for the relaxor ferroelectric properties could be formed [8, 9].

A similar treatment has been applied to the HRTEM image obtained along the [11-2] zone axis (Fig. 3 b) where the period doubling from 0.23 to 0.47 nm along the [111] direction is also visible. The Fourier transform of the HRTEM image (Fig. 5a) is shown in Fig. 5b. As on the corresponding electron diffraction pattern (Fig. 2 b), diffuse spots in the ½ 111 positions are visible. The amplitude image (Fig. 5 c) giving the fringe contrast and ordering degree is obtained by selecting one superstructure spot from the Fourier transform image and back Fourier transform into real space. Just as for the previous zone axis, the amplitude image reveals domains with variable ordering degree (bright = ordered, dark = disordered) with dimensions in the 2-5 nm range.

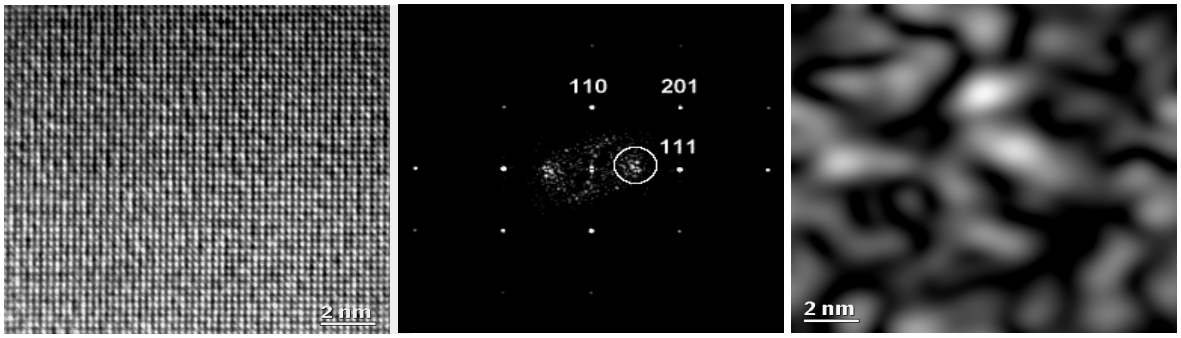

(a) *(b)* *(c)*

Fig. 5. HRTEM image processing for the 0.9PMN -0.1PT sample in the [11-2] orientation: (a) the HRTEM image; (b) FFT of (a); (c) amplitude image obtained from the FFT^{-1} of the distribution in (b) by selecting the diffuse spot in the ½ 111 position.

The origin of the period doubling along the <111> directions in PMN, as revealed by electron diffraction and HRTEM observations, is not yet well understood. In order to identify a possible cause, one has to consider the crystal structure of this compound. PMN has a cubic perovskite structure, with the generic formula ABO_3. In our case, Pb^{2+} cations occupy the A positions, while the B positions are shared by Mg^{2+} (33%) and Nb^{5+} (67%) cations in a disordered matrix (Fig. 6 a). A possible explanation of the period doubling along the <111> directions could be due to Mg^{2+} and Nb^{5+} ordering in successive {111} planes, as schematised in Fig. 6 b. However, an ordered state of this kind would lead to a local stoichiometry with equal content of Mg and Nb, like $PbMg_{0.5}Nb_{0.5}O_3$, meaning regions richer in Mg and poorer in Nb than the theoretical stoichiometry $PbMg_{0.33}Nb_{0.67}O_3$.

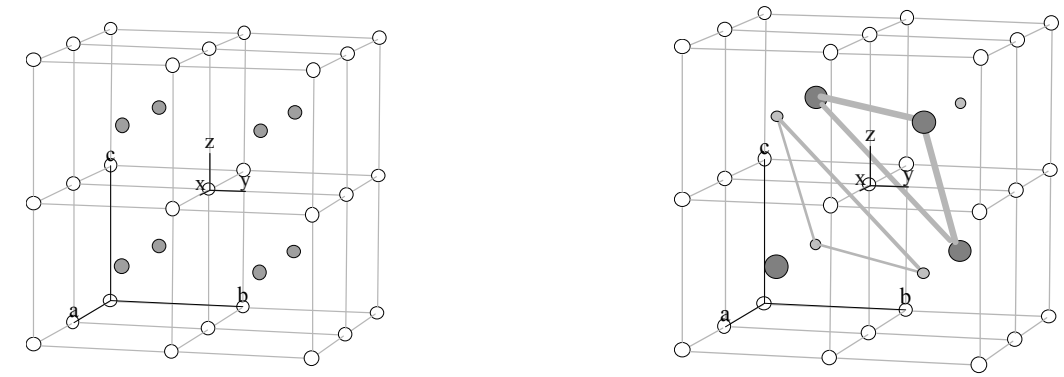

○ Pb^{2+} ions

● Atomic positions ocupied by Mg^{2+} (33%) and Nb^{5+} (67%) in a disordered PMN structured

● Nb^{5+} ions in an ordered PMN structure

○ Mg^{2+} ions in an ordered PMN structure

Fig. 6. PMN crystal structure in disordered (a) and ordered (b) states. The {111} planes occupied by Mg^{2+} and Nb^{5+} are indicated by thick lines. For a better clarity of the structure, the O^{2-} ions situated in the ½ ½ 0 positions are not figured.

Still, this explanation is in rather good agreement with EDS measurements performed on this sample (not shown here), where the detected Mg and Nb concentrations were comparable. For such an interpretation of the superstructure spots, ordered nonstoichiometric domains of $PbMg_{0.5}Nb_{0.5}O_3$ should be immersed in a disordered matrix rich in Nb. Given the valence conditions, an ordered compound of the $Pb^{2+}Mg^{2+}{}_{0.5}Nb^{5+}{}_{0.5}O^{2-}{}_3$ kind is negatively charged, demanding an electrical positive compensation from the disordered Nb-enriched surrounding matrix. The fact that the domains are electrically charged could explain their reduced, nanometric size. Another possibility to maintain the electrical neutrality inside the ordered domains is represented by the formation of oxygen vacancies. This hypothesis should be verified by adequate analysis methods.

Another possible explanation for the presence of the superstructure spots could consist in the formation of domains inside which a rombohedral deformation of the PMN perovskite structure occurs by slight atomic displacements along the <111> directions [10]. EXAFS (*Extended X-ray Absorbtion Fine Structure*) measurements evidenced displacements of about 0.001 nm of the Nb ions inside the NbO_6 octahedra. These atomic displacements lead to the formation of polar aggregates with rombohedral crystallographic symmetry, indicated by X-ray and neutron diffraction [11]. At temperatures lower than 600 K, these displacements are correlated. The correlation range increases with the temperature decrease and, implicitly, the aggregates size which may reach up to 10 nm [12].

4. Conclusion

The TEM/HRTEM study presented in this work revealed the formation of nanometric size domains in $90\%Pb(Mg_{1/3}Nb_{2/3})O_3$ - $10\%PbTiO_2$ ceramic sample. Characteristic diffuse superstructure spots in the ½ 111 positions have been observed on the SAED patterns, indicating the presence of possibly structurally ordered domains with a double cell parameter. HRTEM observations followed by digital image processing have been used in order to visualize the nanodomains. Specialised software routines based on Fourier filtering have been employed.

Amplitude images have been extracted from the experimental HRTEM images, revealing domains with different ordering degrees displayed as levels of gray. The size range of the domains is 2-5 nm, inaccessible to the resolution and contrast limits of the dark field imaging used in conventional electron microscopy. The origin of the observed nanodomains is not yet well understood. It could be either a process of Mg^{2+} / Nb^{5+} ordering in successive {111} planes or a rombohedral deformation of the PMN perovskite structure along the <111> directions.

Acknowledgements

This work is part of the bilateral Flemish - Romanian reserch project BIL 01/73, with support from the Romanian Ministry of Education and Research project CERES C4-76/2004.

References

[1] M. J. Hÿtch, E. Snoeck, R. Kilaas, Ultramicroscopy **74**, 131 (1998).
[2] L. C. Nistor, C. Ghica, G. van Tendeloo, Phys. Stat. Sol. (c) **4** (3), 736 (2007).
[3] C. A. Randall, A. S. Bhalla, Jpn. J. Appl. Phys. **29**, 323 (1990).
[4] C. Tantigate, J. Lee, A. Safari, Appl. Phys. Lett. **66**, 1611 (1995).
[5] A. D. Hilton, C. A. Randall, D. J. Barber and T. R. Shrout, Ferroelectrics **93**, 379 (1989).
[6] O. Bidault, E. Husson and A. Morell, J. Appl. Phys. **82**, 5674 (1997).
[7] P. K. Davies and M. A. Akbas, J. Phys. Chem. Solids **61**, 159 (2000).
[8] A. A. Bokov and Z. -G. Ye, J. Mat. Sci. **41**, 31 (2006).
[9] E. C. Colla, N. K. Yushin, D. Viehland, J. Appl. Phys. **83**, 3294 (1998).
[10] E. Prouzet, E. Husson, N. de Mathan, A. Morell, J. Phys.: Condens. Matter. **5**, 4889 (1991).
[11] E. Prouzet, E. Husson, N. de Mathan, A. Morell, J. Phys.: Condens. Matter. **5**, 4881 (1991).
[12] N. de Mathan, E. Husson, G. Calvarin, J.R. Gavarri, A. W. Hewat, A. Morell, J. Phys.: Condens. Matter. **3**, 8159 (1991).

*Corresponding author: cghica@infim.ro